PHYSICAL REVIEW D **92,** 094017 (2015)

Photoproduction of the charged charmoniumlike $Z_c^+(4200)$

Xiao-Yun Wang,[1,2,3,*] Xu-Rong Chen,[1,3] and Alexey Guskov[4,†]

[1]*Institute of Modern Physics, Chinese Academy of Sciences, Lanzhou 730000, China*
[2]*University of Chinese Academy of Sciences, Beijing 100049, China*
[3]*Research Center for Hadron and CSR Physics, Institute of Modern Physics of CAS and Lanzhou University, Lanzhou 730000, China*
[4]*Joint Institute for Nuclear Research, Dubna 141980, Russia*

(Received 20 March 2015; published 10 November 2015)

In this work, inspired by the observation of charmoniumlike $Z_c^+(4200)$, we study the photoproduction of charged charmoniumlike $Z_c^+(4200)$ with an effective Lagrangian approach and the Regge trajectories model. The numerical results indicate that the Reggeized treatment can lead to a lower total cross section of the $Z_c^+(4200)$ photoproduction and the peak position of the cross section was moved to the higher energy point when the Reggeized treatment was added. Moreover, by using the data from the COMPASS experiment and presented theoretical predictions, an upper limit of the decay width of $Z_c(4200) \to J/\psi\pi$ is estimated. The relevant results not only shed light on the further experiment of searching for the charmoniumlike $Z_c(4200)$ state via meson photoproduction, but also provide valuable information for having a better comprehension of the nature of a charmoniumlike $Z_c(4200)$ state.

DOI: 10.1103/PhysRevD.92.094017 PACS numbers: 13.60.Le, 11.10.Ef, 11.55.Jy, 12.40.Vv

I. INTRODUCTION

As of now, most hadrons can be well described by the classical constituent quark model in the picture of $q\bar{q}$ for mesons and qqq for baryons. However, according to quantum chromodynamics, exotic states (such as multiquark states, molecule states, etc.) are also allowed to exist in our Universe. Therefore, searching for and explaining these exotic states arouse great interest among researchers.

In the experiments, a series of charmoniumlike and bottomoniumlike states referred to as XYZ have been observed [1–16]. Especially, those charged Z states are even more exotic, since they have a minimal quark content of $|c\bar{c}u\bar{d}\rangle$ (Z_c^+) or $|b\bar{b}u\bar{d}\rangle$ (Z_b^+) [17–21]. Later, some neutral Z states [including $Z_c^0(3900)$, $Z_b^0(10610)$, and $Z_c^0(4020)$] were reported by experiments [22–24], which provide important information for confirming and understanding the exotic Z states.

On theoretical aspects, these exotic states are interpreted as a hadronic molecule, a tetraquark, hadrocharmonium, or just a cusp effect [17–21,25–43]. Moreover, several hidden charm baryons composed by $|c\bar{c}qqq\rangle$ have been predicted and investigated [44–47]. These studies enriched the picture of exotic states.

Recently, the Belle Collaboration claimed that a new charged charmoniumlike $Z_c^+(4200)$ was observed in the invariant mass spectrum of $J/\psi\pi^+$ with a significance of 6.2σ [13]. Its mass and width are $M_{Z_c(4200)} = 4196^{+31+17}_{-29-13}$ MeV/c^2 and $\Gamma_{Z_c(4200)} = 370^{+70+70}_{-70-132}$ MeV [13], respectively. Meanwhile, the quantum number of $Z_c^+(4200)$ was determined to be $J^P = 1^+$, since other hypotheses with $J^P \in \{0^-, 1^-, 2^-, 2^+\}$ were excluded [13]. In Ref. [40], the calculations show that $Z_c(4200)$ is a strong candidate of the lowest axial-vector tetraquark state within the framework of the color-magnetic interaction. In Refs. [41–43], using the QCD sum rule approach, the relevant results also support the tetraquark interpretation of $Z_c(4200)$. Besides, the $Z_c(4200)$ was described as a moleculelike state in Ref. [48]. The above information indicates that $Z_c(4200)$ is an ideal candidate for investigating the nature of exotic charmoniumlike states.

As of now, the charmoniumlike XYZ states are observed in only four ways [17], i.e., the e^+e^- annihilation ($e^+e^- \to XYZ$ or $e^+e^- \to J/\psi + XYZ$), $\gamma\gamma$ fusion process ($\gamma\gamma \to XYZ$), B meson decay ($B \to K + XYZ$), and hidden-charm dipion decays of higher charmonia or charmoniumlike states. Therefore, searching for the charmoniumlike states through other production processes is an important topic, which will be useful in confirming and understanding these exotic XYZ states. For example, Ke and Liu suggested to search for the charged $Z_c^\pm(4430)$ by the nucleon-antinucleon scattering [49], while the production of neutral $Z_c^0(4430)$ and $Z_c^0(4200)$ states in $\bar{p}p$ reaction was investigated in Refs. [50,51]. Moreover, in Refs. [52–55], the meson photoproduction process was proposed to be an effective way to search for the charmoniumlike states. Soon after, according to the theoretical predictions obtained in Ref. [54], an experiment of searching for $Z_c^\pm(3900)$ through $\gamma N \to Z_c^\pm(3900)N \to J/\psi\pi^\pm N$ was carried out by the COMPASS Collaboration [56]. Unfortunately, no signal of exclusive photoproduction of the $Z_c^\pm(3900)$ state and its decay into $J/\psi\pi^\pm$ was found. Thus, it is important to discuss whether there are other charmoniumlike states that

*xywang@impcas.ac.cn
†avg@jinr.ru

have a discovery potential through the $\gamma N \to J/\psi\pi^{\pm}N$ channel. Besides, a more accurate theoretical prediction is necessary.

Usually, for the meson photoproduction process, the mesonic Reggeized treatment will play important role at high photoenergies. The exchange of dominant meson Regge trajectories has already been used to successfully describe meson photoproduction in Refs. [57–59]. Since a high photon beam energy is required for the production of charmoniumlike states through the meson photoproduction process, the Reggeized treatment will be necessary to ensure the result's accuracy. In this work, within the frame of an effective Lagrangian approach and the Regge trajectories model, we systematically study the production of charged $Z_c(4200)$ by the meson photoproduction process in order to provide a reliable theoretical result and shed light on our understanding of the properties and production mechanism of a charged $Z_c(4200)$ state.

This paper is organized as follows. After an introduction, we present the investigation method and formalism. The numerical result and discussion are given in Sec. III. In Sec. IV, we discuss the upper limit of decay width of $Z_c(4200) \to J/\psi\pi$. Finally, this paper ends with a brief conclusion.

II. FORMALISM AND INGREDIENTS

Since $Z_c(4200)$ has a strong coupling with $J/\psi\pi$ [13,40,43], the photoproduction process $\gamma p \to Z_c^+(4200)n \to J/\psi\pi^+ n$ may be an ideal reaction channel for searching and studying production of the charged $Z_c^+(4200)$. Moreover, considering the signal of $Z_c^+(4200)$ is mainly from the contributions of π exchange, while the contributions from ρ and a_0 exchange can be negligible,[1] the process as depicted in Fig. 1 is regarded as the source of the signal of $Z_c^+(4200)$. Besides, the reaction $\gamma p \to J/\psi\pi^+ n$ via Pomeron exchange (as shown in Fig. 2) is also calculated, which is considered to be the background for $Z_c^+(4200)$ photoproduction. To investigate $Z_c^+(4200)$ production, an effective Lagrangian approach and the Regge trajectories model in terms of hadrons will be used in the following.

A. Feynman diagrams and effective interaction Lagrangian densities

Figure 1 show the basic tree-level Feynman diagram for the production of $Z_c^+(4200)$ in a $\gamma p \to Z_c^+(4200)n \to J/\psi\pi^+ n$ reaction via pion exchange. To gauge the

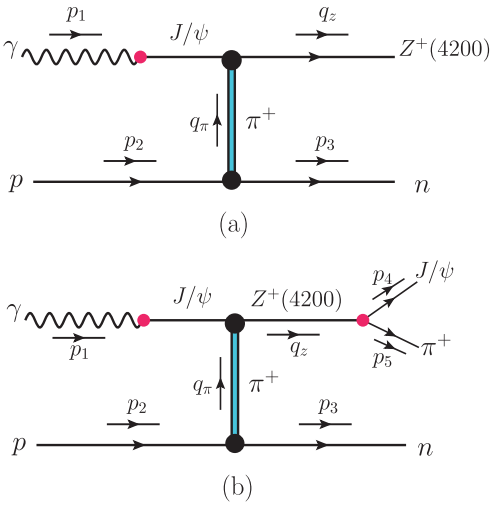

FIG. 1 (color online). The Feynman diagram for a $\gamma p \to Z_c^+(4200)n$ reaction (a) and a $\gamma p \to J/\psi\pi^+ n$ reaction (b) through π exchange.

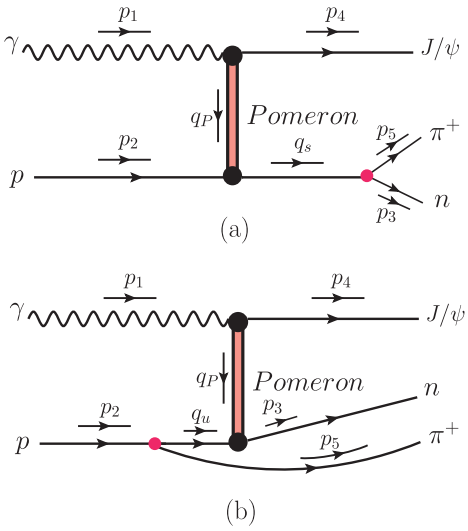

FIG. 2 (color online). The Feynman diagram of the $\gamma p \to J/\psi\pi^+ n$ process through Pomeron exchange.

contributions of these diagrams, we need to know the effective Lagrangian densities for each interaction vertex.

For the interaction vertex of πNN, we use the effective pseudoscalar coupling[2] [68–70]

$$\mathcal{L}_{\pi NN} = -ig_{\pi NN}\bar{N}\gamma_5\vec{\tau}\cdot\vec{\pi}N, \quad (1)$$

[1]In Refs. [60–62], the results indicate that the pion exchange plays a major role in the $\gamma p \to Xn$ process by analyzing the HERA data. Besides, in Refs. [63,64], it is found that the contributions of ρ and a_0 exchange in the $\gamma^* p \to Xn$ reaction are very small. Thus, in the present work, we consider only the contribution from the one-pion exchange. Here, the γ^* stand for the virtual photon.

[2]It should be noted that some works [65,66] have pointed out that the simple pseudoscalar coupling between nucleons and pions is incomplete and inconsistent with chiral symmetry. Thus, pseudovector coupling is suggested in Refs. [65,66]. However, since the new pseudovector formalism may not yet be ready for phenomenological use [67], pseudoscalar coupling is adopted in the present work.

where N and π stand for the fields of the nucleon and pion meson, respectively, while $\vec{\tau}$ is the Pauli matrix. The coupling constant of the πNN interaction was given in many theoretical works, and we take $g^2_{\pi NN}/4\pi = 14.4$ [71].

As mentioned above, the spin parity of $Z_c^+(4200)$ has been determined by the Belle Collaboration to be $J^P = 1^+$ [13]. Thus, the relevant effective Lagrangian for the vertex[3] of $Z\psi\pi$ reads as [52]

$$\mathcal{L}_{Z\psi\pi} = \frac{g_{Z\psi\pi}}{M_Z}(\partial^\mu\psi^\nu\partial_\mu\pi Z_\nu - \partial^\mu\psi^\nu\partial_\nu\pi Z_\mu), \tag{2}$$

where Z and ψ denote the fields of the $Z(4200)$ and J/ψ meson, respectively. With the effective Lagrangians above, the coupling constant $g_{Z\psi\pi}$ can be determined by the partial decay widths $\Gamma_{Z_c(4200)\to J/\psi\pi}$:

$$\Gamma_{Z(4200)\to J/\psi\pi} = \left(\frac{g_{Z\psi\pi}}{M_Z}\right)^2 \frac{|\vec{p}_\pi^{\,\text{c.m.}}|}{24\pi M_Z^2} \times \left[\frac{(M_Z^2 - m_\psi^2 - m_\pi^2)^2}{2} + m_\psi^2 E_\pi^2\right], \tag{3}$$

with

$$|\vec{p}_\pi^{\,\text{c.m.}}| = \frac{\lambda^{1/2}(M_Z^2, m_\psi^2, m_\pi^2)}{2M_Z}, \tag{4}$$

$$E_\pi = \sqrt{|\vec{p}_\pi^{\,\text{c.m.}}|^2 + m_\pi^2}, \tag{5}$$

where λ is the Källen function with $\lambda(x,y,z) = (x-y-z)^2 - 4yz$.

As of now, no relevant experiment data about $\Gamma_{Z(4200)\to J/\psi\pi}$ can be available [72]. However, in Ref. [43], the authors obtained the partial decay width $\Gamma_{Z_c(4200)\to J/\psi\pi} = 87.3 \pm 47.1$ MeV with the QCD sum rule approach, which allows us to estimate the lower (upper) limit of the decay width of $Z(4200) \to J/\psi\pi$, $\Gamma_{Z(4200)\to J/\psi\pi} = 40.2(134.4)$ MeV. With $M_Z = 4196$ MeV$/c^2$ and $\Gamma_Z = 370$ MeV [72], we get $g_{Z\psi\pi}/M_z = 1.174$, 1.731, and 2.147 MeV, which correspond to three typical partial decay width $\Gamma_{Z(4200)\to J/\psi\pi} = 40.2$, 87.3, and 134.4 MeV, respectively.

For the interaction vertex of $Z\gamma\pi$, we need to derive it by the vector meson dominance (VMD) mechanism [73–75]. In the VMD mechanism for photoproduction, a real photon can fluctuate into a virtual vector meson, which subsequently scatters off the target proton. Thus, within the frame of the VMD mechanism, we get the Lagrangian of depicting the coupling of the intermediate vector meson J/ψ with a photon as follows:

[3]For the sake of simplicity, we use Z and ψ to denote $Z_c(4200)$ and J/ψ, respectively.

$$\mathcal{L}_{J/\psi\gamma} = -\frac{em_\psi^2}{f_\psi}V_\mu A^\mu, \tag{6}$$

where m_ψ^2 and f_ψ are the mass and the decay constant of the J/ψ meson, respectively. With the above equation, one gets the expression for the $J/\psi \to e^+e^-$ decay:

$$\Gamma_{J/\psi\to e^+e^-} = \left(\frac{e}{f_\psi}\right)^2 \frac{8\alpha|\vec{p}_e^{\,\text{c.m.}}|^3}{3m_\psi^2}, \tag{7}$$

where $\vec{p}_e^{\,\text{c.m.}}$ indicates the three-momentum of an electron in the rest frame of the J/ψ meson, while $\alpha = e^2/4\hbar c = 1/137$ is the electromagnetic fine structure constant. Thus, in light of the partial decay width of $J/\psi \to e^+e^-$ [72]

$$\Gamma_{J/\psi\to e^+e^-} \simeq 5.547 \text{ keV}, \tag{8}$$

we get the constant $e/f_\psi \simeq 0.027$.

In Fig. 2, we present the Feynman diagram for the $\gamma p \to J/\psi\pi^+ n$ process through Pomeron exchange, which is considered as the main background contributions to the $\gamma p \to Z_c^+(4200)n \to J/\psi\pi^+ n$ process. To depict the Pomeron exchange process, the relevant formulas which were used in Refs. [52,76,77] are adopted in this work. The Pomeron-nucleon coupling is described as follows:

$$F_\mu(t) = \frac{3\beta_0(4m_N^2 - 2.8t)}{(4m_N^2 - t)(1 - t/0.7)^2}\gamma_\mu = F(t)\gamma_\mu, \tag{9}$$

where $t = q_P^2$ is the exchanged Pomeron momentum squared. $\beta_0^2 = 4$ GeV^2 stands for the coupling constant between a single Pomeron and a light constituent quark.

For the vertex of $\gamma\psi\mathcal{P}$, with an on-shell approximation for keeping the gauge invariance, we have

$$V_{\gamma\psi\mathcal{P}} = \frac{2\beta_c \times 4\mu_0^2}{(m_\psi^2 - t)(2\mu_0^2 + m_\psi^2 - t)} T_{\mu\rho\nu}\epsilon_\psi^\nu \epsilon_\gamma^\mu \mathcal{P}^\rho, \tag{10}$$

with

$$T^{\mu\rho\nu} = (p_1 + p_4)^\rho g^{\mu\nu} - 2p_1^\nu g^{\rho\mu} + 2\left\{p_1^\mu g^{\rho\nu} + \frac{p_4^\nu}{p_4^2}(p_1\cdot p_4 g^{\rho\mu} - p_1^\rho p_4^\mu - p_1^\mu p_4^\rho) - \frac{p_1^2 p_4^\mu}{p_4^2 p_1\cdot p_4}(p_4^2 g^{\rho\nu} - p_4^\rho p_4^\nu)\right\} + (p_1 - p_4)^\rho g^{\mu\nu}, \tag{11}$$

where $\beta_c^2 = 0.8$ GeV^2 is the effective coupling constant between a Pomeron and a charm quark within the J/ψ meson, while $\mu_0 = 1.2$ GeV^2 denotes a cutoff parameter in the form factor of a Pomeron.

B. Cross sections for the $\gamma p \to Z_c^+(4200)n$ reaction

After the above preparations, the invariant scattering amplitude $\mathcal{A}$ for the $\gamma(p_1)p(p_2) \to Z_c^+(4200)(q_z)n(p_3)$ reaction by exchanging a π meson reads as

$$\begin{aligned}\mathcal{A} = &\left(\sqrt{2}g_{\pi NN}\frac{g_{Z\psi\pi}}{M_Z}\frac{e}{f_\psi}\right)\bar{u}(p_3)\gamma_5 u(p_2)\epsilon_Z^{*\mu} \\ &\times \epsilon_\gamma^\nu[p_1\cdot(q_z-p_1)g_{\mu\nu} - p_{1\mu}(q_z-p_1)_\nu] \\ &\times \frac{1}{q_\pi^2 - m_\pi^2}F_{\pi NN}(q_\pi^2)F_{Z\psi\pi}(q_\pi^2),\end{aligned} \tag{12}$$

where $F_{\pi NN}(q_\pi^2)$ and $F_{Z\psi\pi}(q_\pi^2)$ are the form factors for the vertices of πNN and $Z\psi\pi$, respectively. We have the following definitions for both form factors:

$$F_{\pi NN}(q_\pi^2) = \frac{\Lambda_\pi^2 - m_\pi^2}{\Lambda_\pi^2 - q_\pi^2} \tag{13}$$

and

$$F_{Z\psi\pi}(q_\pi^2) = \frac{m_\psi^2 - m_\pi^2}{m_\psi^2 - q_\pi^2}, \tag{14}$$

where Λ_π is the cutoff parameter for the πNN vertex. In the next calculations, we take the typical value of $\Lambda_\pi = 0.7$ GeV as used in Refs. [52,54,58,78].

As mentioned above, a higher photon beam energy is required for the production of charmoniumlike states through the meson photoproduction process. Thus, to better describe the photoproduction of $Z_c^+(4200)$ at high photon energies, we introduce a pion Reggeized treatment by replacing the Feynman propagator $\frac{1}{q_\pi^2 - m_\pi^2}$ with the Regge propagator as follows [57–59,79]:

$$\frac{1}{q_\pi^2 - m_\pi^2} \to \mathcal{R}_\pi = \left(\frac{s}{s_{\rm scale}}\right)^{\alpha_\pi(t)}\frac{\pi\alpha_\pi'}{\Gamma[1+\alpha_\pi(t)]}\frac{e^{-i\pi\alpha_\pi(t)}}{\sin[\pi\alpha_\pi(t)]}, \tag{15}$$

where α_π' is the slope of the trajectory and the scale factor $s_{\rm scale}$ is fixed at 1 GeV^2, while $s = (p_1+p_2)^2$ and $t = (p_2+p_3)^2$ are the Mandelstam variables. In addition, the pionic Regge trajectory $\alpha_\pi(t)$ reads as [58,59,79]

$$\alpha_\pi(t) = 0.7(t - m_\pi^2). \tag{16}$$

The unpolarized differential cross section for the $Z_c^+(4200)$ photoproduction shown in Fig. 1(a) then reads

$$\frac{d\sigma}{d\cos\theta} = \frac{1}{32\pi s}\frac{|\vec{q}_z^{\,\rm c.m.}|}{|\vec{p}_1^{\,\rm c.m.}|}\left(\frac{1}{4}\sum_{\rm spins}|\mathcal{A}|^2\right), \tag{17}$$

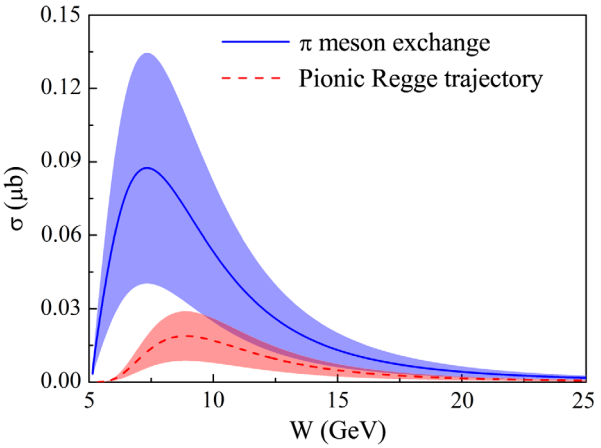

FIG. 3 (color online). The total cross section for the $\gamma p \to Z_c^+(4200)n$ process through π meson or pionic Regge trajectory exchange. Here, the numerical results (the blue solid line and the red dashed line) correspond to the partial decay width $\Gamma_{Z_c(4200)\to J/\psi\pi} = 87.3$ MeV, while the bands stand for the uncertainties with the variation of $\Gamma_{Z_c(4200)\to J/\psi\pi}$ from 40.2 to 131.4 MeV.

where $\vec{p}_1^{\,\rm c.m.}$ and $\vec{q}_z^{\,\rm c.m.}$ are the three-momentum of the initial photon and final $Z_c^+(4200)$ state, respectively, while θ denotes the angle of the outgoing $Z_c^+(4200)$ state relative to the photon beam direction in the c.m. frame. The total cross section can be easily obtained by integrating the above equation.

In Fig. 3, the total cross section $\sigma(\gamma p \to Z_c^+ n)$ through π meson or pionic Regge trajectory exchange is presented with $\Lambda_\pi = 0.7$ GeV. Since the total cross section is proportional to the partial decay width $\Gamma_{Z(4200)\to J/\psi\pi}$, we note that the cross section changes by a factor of 3–4 when the partial width $\Gamma_{Z(4200)\to J/\psi\pi}$ is varied from 40.2 to 134.4 MeV. Besides, it is found that the total cross section through the Reggeized treatment is about 5 times smaller than that of the result through a π exchange, which indicates that the Reggeized treatment can lead to a lower cross section of $Z_c^+(4200)$ photoproduction at high photon energies. Moreover, we note that the peak position of the total cross section was moved to the higher energy point when the Reggeized treatment is used in the calculations.

Figure 4 shows the differential cross section for the $\gamma p \to Z_c^+ n$ process by exchanging the π meson or pionic Regge trajectory at different energies, respectively. From Fig. 4, one can see that, relative to the results related to the π exchange, the differential cross section by exchanging the pionic Regge trajectory is very sensitive to the θ angle and gives a considerable contribution at forward angles.

C. Cross sections for the $\gamma p \to J/\psi\pi^+ n$ reaction

With the Feynman rules and above Lagrangian densities, we obtain the invariant scattering amplitude $\mathcal{M}_Z^{\rm signal}$ for the

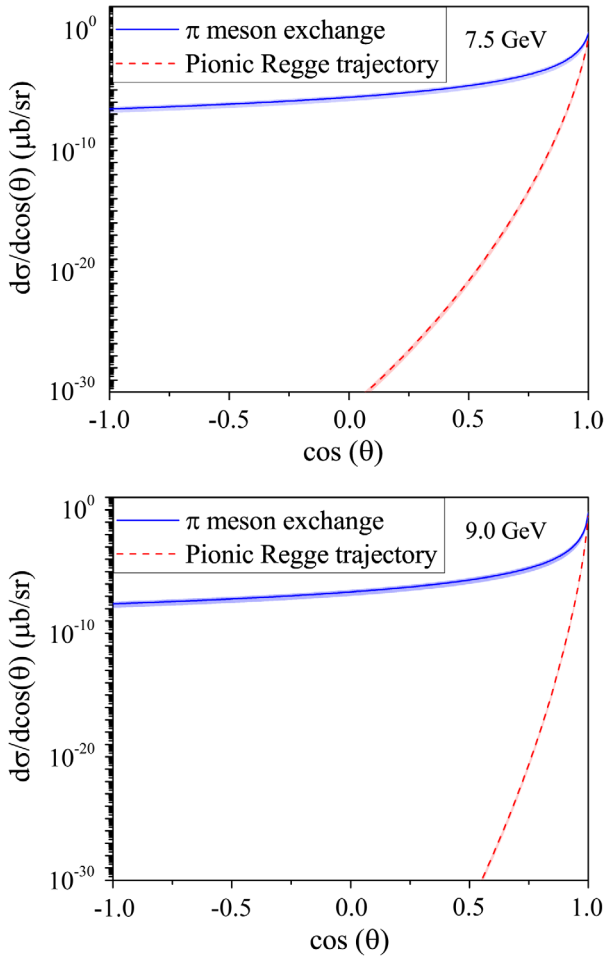

FIG. 4 (color online). The differential cross section for the $\gamma p \to Z_c^+(4200)n$ process through π meson or pionic Regge trajectory exchange. The notation of the lines and bands is as in Fig. 3.

$\gamma p \to J/\psi\pi^+ n$ process through π exchange [as depicted in Fig. 1(b)] as follows:

$$\begin{aligned}\mathcal{M}_Z^{\text{signal}} =& \left(\sqrt{2}g_{\pi NN}\frac{g_{Z\psi\pi}}{M_Z}\frac{e}{f_\psi}\right)\bar{u}(p_3)\gamma_5 u(p_2)\\ &\times (p_1\cdot q_\pi g^{\mu\alpha} - p_1^\alpha q_\pi^\mu)(p_4\cdot p_5 g^{\rho\nu} - p_4^\rho p_5^\nu)\\ &\times \frac{1}{q_\pi^2 - m_\pi^2} G_Z^{\rho\alpha}(q_z)\epsilon_{\gamma\mu}\epsilon_{\psi\nu}^*\left(\frac{\Lambda_\pi^2 - m_\pi^2}{\Lambda_\pi^2 - q_\pi^2}\right)\\ &\times \left(\frac{m_\psi^2 - m_\pi^2}{m_\psi^2 - q_\pi^2}\right)\left(\frac{m_\psi^2 - M_Z^2}{m_\psi^2 - q_z^2}\right),\end{aligned} \tag{18}$$

where $G_Z^{\mu\alpha}$ are the propagators of the $Z(4200)$, taking the Breit-Wigner form [80]

$$G_Z^{\rho\alpha}(q) = \frac{-g_{\rho\alpha} + q_{z\rho}q_{z\alpha}/M_Z^2}{q_z^2 - M_Z^2 + iM_Z\Gamma_Z}. \tag{19}$$

Just as above, by replacing the Feynman propagator $\frac{1}{q_\pi^2 - m_\pi^2}$ with the Regge propagator $\mathcal{R}_\pi$, we can get the scattering amplitude for the $\gamma p \to J/\psi\pi^+ n$ process through the pionic Regge trajectory exchange.

Since the Pomeron can mediate the long-range interaction between a confined quark and a nucleon, $\gamma p \to J/\psi\pi^+ n$ via the Pomeron exchange (as described in Fig. 2) are the mainly background contribution to the $\gamma p \to Z_c^+(4200)n \to J/\psi\pi^+ n$ reaction. The invariant scattering amplitudes $\mathcal{M}_P^s$ and $\mathcal{M}_P^u$ for Figs. 2(a) and 2(b) can be written, respectively, as

$$\begin{aligned}\mathcal{M}_P^s =& 8\sqrt{2}\beta_c\mu_0^2 g_{\pi NN}F_N(q_s^2)\frac{F(t)G_P(s,t)}{(m_\psi^2 - t)(2\mu_0^2 + m_\psi^2 - t)}\\ &\times T^{\mu\rho\nu}\epsilon_{\psi\nu}^*\epsilon_{\gamma\mu}\bar{u}(p_3)\gamma_5\frac{\not{q}_s + m_N}{q_s^2 - m_N^2}\gamma_\rho u(p_2),\end{aligned} \tag{20}$$

$$\begin{aligned}\mathcal{M}_P^u =& 8\sqrt{2}\beta_c\mu_0^2 g_{\pi NN}F_N(q_u^2)\frac{F(t)G_P(s,t)}{(m_\psi^2 - t)(2\mu_0^2 + m_\psi^2 - t)}\\ &\times T^{\mu\rho\nu}\epsilon_{\psi\nu}^*\epsilon_{\gamma\mu}\bar{u}(p_3)\gamma_\rho\frac{\not{q}_u + m_N}{q_u^2 - m_N^2}\gamma_5 u(p_2)\end{aligned} \tag{21}$$

with

$$G_P(s,t) = -i(\eta' s)^{\eta(t)-1}, \tag{22}$$

where $\eta(t) = 1 + \epsilon + \eta' t$ is the Pomeron trajectory. Here, the concrete values $\epsilon = 0.08$ and $\eta' = 0.25$ GeV^{-2} are adopted.

Considering the size of the hadrons, the monopole form factor for the off-shell intermediate nucleon is introduced as in the Bonn potential model [81]:

$$F_N(q_i^2) = \frac{\Lambda_N^2 - m_N^2}{\Lambda_N^2 - q_i^2}, \qquad i = s, u, \tag{23}$$

where Λ_N and $q_i (q_s = p_3 + p_5, q_u = p_2 - p_5)$ are the cutoff parameter and four-momentum of the intermediate nucleon, respectively. For the value of Λ_N, we will discuss it in the next section. It is worth mentioning that the form factor is phenomenological and has a great uncertainty. Thus, the dipole form factor deserves to be discussed and compared with the monopole form.

Combining the signal terms and background amplitudes, we get the total invariant amplitude

$$\mathcal{M} = \mathcal{M}_Z^{\text{signal}} + \mathcal{M}_P^s + \mathcal{M}_P^u. \tag{24}$$

Thus, the total cross section of the $\gamma p \to J/\psi\pi^+ n$ reaction could be obtained by integrating the invariant amplitudes in the three-body phase space:

$$d\sigma(\gamma p \to J/\psi\pi^+ n) = \frac{m_N^2}{|p_1 \cdot p_2|}\left(\frac{1}{4}\sum_{\text{spins}}|\mathcal{M}|^2\right) \times (2\pi)^4 d\Phi_3(p_1+p_2; p_3, p_4, p_5), \quad (25)$$

where the three-body phase space is defined as [72]

$$d\Phi_3(p_1+p_2; p_3, p_4, p_5) = \delta^4\left(p_1+p_2-\sum_{i=3}^{5} p_i\right)\prod_{i=3}^{5}\frac{d^3p_i}{(2\pi)^3 2E_i}. \quad (26)$$

III. NUMERICAL RESULTS AND DISCUSSION

With the FOWL code in the CERN program library, the total cross section including both signal and background contributions can be calculated. In these calculations, the cutoff parameter Λ_N related to the Pomeron term is a free parameter. Thus, we first need to give a constraint on the value of Λ_N. Figures 5(a) and 5(b) present the variation of the cross section from the background contributions for $\gamma p \to J/\psi\pi^+ n$ with a monopole and dipole form factor, respectively. It is obvious that the Pomeron exchange contributions with a dipole form factor are more sensitive to the values of the cutoff Λ_N than that of a monopole form factor. Thus, the monopole form factor is adopted in the following calculation.

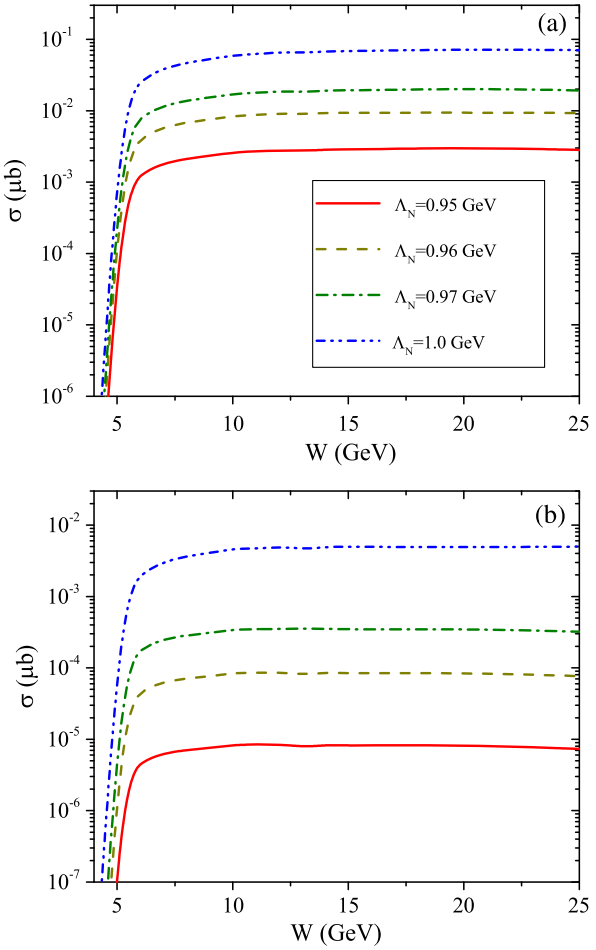

FIG. 5 (color online). (a) The cross section of background from the Pomeron exchange for the $\gamma p \to J/\psi\pi^+ n$ process with a monopole form factor at the different values of the cutoff parameter Λ_N. (b) is the same as (a), but for the case of a dipole form factor.

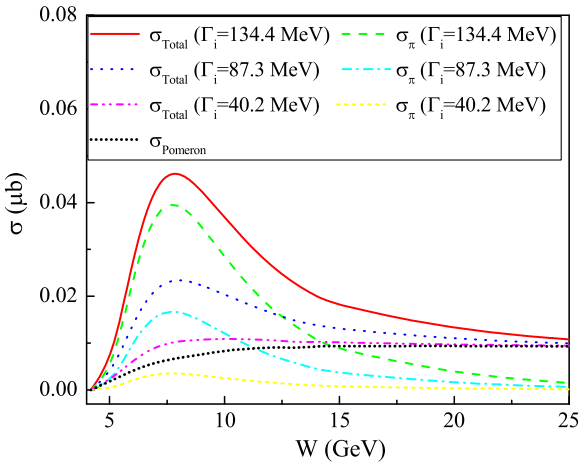

FIG. 6 (color online). The energy dependence of the total cross sections for the $\gamma p \to J/\psi\pi^+ n$ reaction. Here, σ_{Pomeron} and σ_π denote the results via the Pomeron and π exchange, respectively, while σ_{Total} is the total cross section of $\gamma p \to J/\psi\pi^+ n$. The variations of σ_π and σ_{Total} to W with several typical partial width values $\Gamma_{Z(4200)\to J/\psi\pi} = 40.2$, 87.3, and 134.4 MeV are also presented.

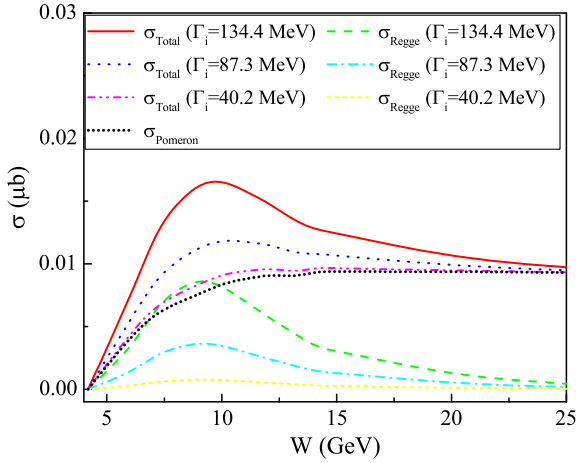

FIG. 7 (color online). The energy dependence of the total cross sections for the $\gamma p \to J/\psi\pi^+ n$ reaction. Here, σ_{Pomeron} and σ_{Regge} denote the results via the Pomeron exchange and pionic Regge trajectory exchange, respectively, while σ_{Total} is the total cross section of $\gamma p \to J/\psi\pi^+ n$. The variations of σ_{Regge} and σ_{Total} to W with several typical partial width values $\Gamma_{Z(4200)\to J/\psi\pi} = 40.2$, 87.3, and 134.4 MeV are also presented.

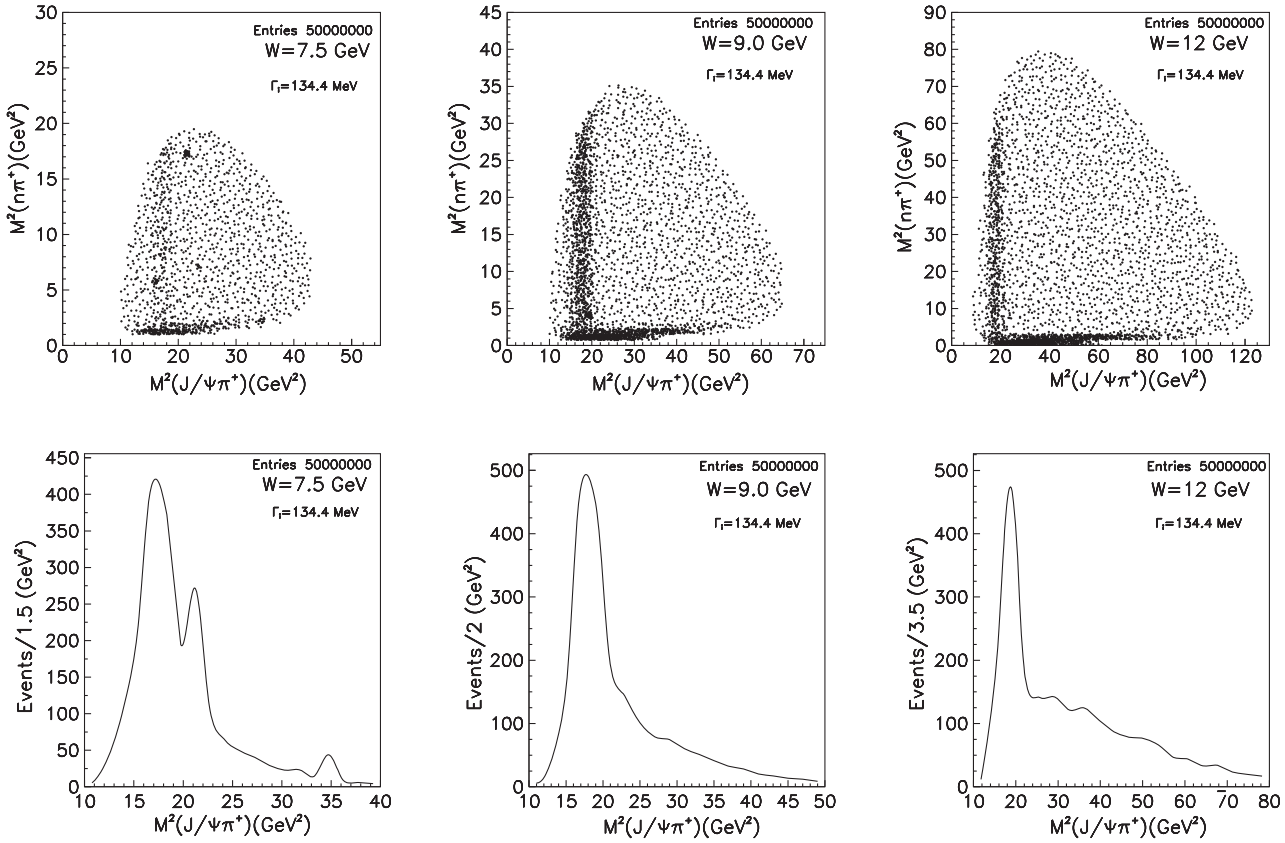

FIG. 8. The Dalitz plot (top) and the $J/\psi\pi^+$ invariant mass spectrum (bottom) for the $\gamma p \to J/\psi\pi^+ n$ reaction with the Reggeized treatment at different center-of-mass energies $W = 7.5$, 9, and 12 GeV. Here, the numerical result corresponds to the partial decay width $\Gamma_{Z(4200)\to J/\psi\pi} = 134.4$ MeV.

At present, no experiment data are available for the $\gamma p \to J/\psi\pi^+ n$ process. However, we notice that the similar reactions $\gamma p \to J/\psi p$ and $\bar{p}p \to J/\psi\pi^0$ have been measured by some experiments [82–85], where the measured cross sections of these two process are about 1 and 10 nb, respectively. Here, we naively think that the cross section of $\gamma p \to J/\psi\pi^+ n$ may be equal to or less than that of $\gamma p \to J/\psi p$, while it is greater than that of $\bar{p}p \to J/\psi\pi^0$. Thus, we constrain the cutoff to be $\Lambda_N = 0.96$ GeV as used in Refs. [54,55], which will be used in our calculations.

To better understand the effects of Reggeized treatment on the final results, we calculate the total cross section of the $\gamma p \to J/\psi\pi^+ n$ reaction without or with Reggeized treatment as presented in Figs. 6 and 7, respectively.

Figure 6 shows the total cross sections for the $\gamma p \to J/\psi\pi^+ n$ reaction including both π exchange and Pomeron exchange contributions by taking $\Lambda_Z = 0.7$ GeV and $\Lambda_N = 0.96$ GeV. We notice that the line shape of the total cross section goes up very rapidly and has a peak around $W \simeq 7.5$ GeV. In this energy region, the cross section of the signal is larger than that of the background when taking the partial width values $\Gamma_{Z_c(4200)\to J/\psi\pi} = 87.3$ or 134.4 MeV.

In contrast, Fig. 7 presents the total cross sections for the $\gamma p \to J/\psi\pi^+ n$ reaction including both pionic Regge trajectory exchange and Pomeron exchange contributions by taking $\Lambda_Z = 0.7$ GeV and $\Lambda_N = 0.96$ GeV. It is found that the total cross section shows a peak at center-of-mass energy $W \simeq 9$ GeV, and the contributions from the signal are driven down when using the Reggeized treatment. We note that for the cross section of the signal just a little bit higher than that of the background at center-of-mass energy $W \simeq 9$ GeV even a larger partial decay width value ($\Gamma_{Z_c(4200)\to J/\psi\pi} = 134.4$ MeV) is adopted.

To demonstrate the feasibility of searching for the charged charmoniumlike $Z_c^+(4200)$ through the $\gamma p \to J/\psi\pi^+ n$ reaction, we further give the Dalitz plot and invariant mass spectrum for the $\gamma p \to J/\psi\pi^+ n$ process.

Figure 8 presents the Dalitz plot and $J/\psi\pi^+$ invariant mass spectrum for the $\gamma p \to J/\psi\pi^+ n$ process with the Reggeized treatment at different center-of-mass energies, where the numerical results are obtained by taking the partial decay width $\Gamma_{Z_c(4200)\to J/\psi\pi} = 134.4$ MeV. From the Dalitz plot we notice that there exist a vertical band and a horizontal band, which are from the signal and background contributions, respectively. Moreover, one notices that the signal of $Z_c^+(4200)$ with $W = 9.0$ is more explicit than that with

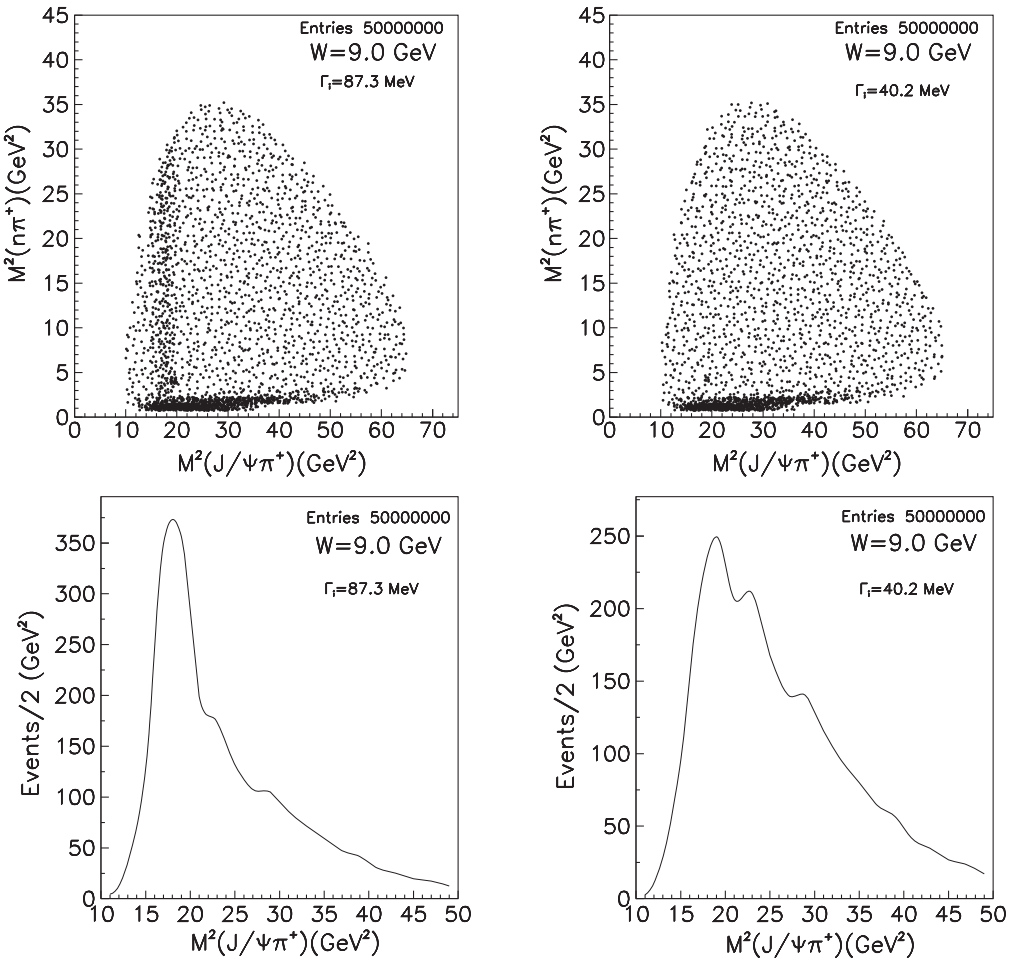

FIG. 9. The Dalitz plot (top) and the $J/\psi\pi^+$ invariant mass spectrum (bottom) for the $\gamma p \to J/\psi\pi^+ n$ reaction with the Reggeized treatment at center-of-mass energy $W = 9$ GeV. Here, the numerical results correspond to the partial decay width values $\Gamma_{Z(4200)\to J/\psi\pi} = 87.3$ and 40.2 MeV.

$W = 7.5$ or 12 GeV, which is consistent with the result in Fig. 7. Thus, we can conclude that $W = 9.0$ GeV is the best energy window for searching for the charged $Z_c^+(4200)$ via the $\gamma p \to J/\psi\pi^+ n$ process. By analyzing the $J/\psi\pi^+$ invariant mass spectrum in Fig. 8, one finds that the number of events of $J/\psi\pi^+$ can reach up to $500/2$ GeV^2 at $W = 9.0$ GeV when taking 50×10^6 collisions of γp.

Moreover, we take the center-of-mass energy $W = 9.0$ GeV as one of the inputs to calculate the Dalitz plot and $J/\psi\pi^+$ invariant mass spectrum related to the smaller partial decay width, which are presented in Fig. 9. From the Dalitz plot in Fig. 9, we notice that there exists a clear vertical band which is related to the $Z_c^+(4200)$ signal when taking partial decay width $\Gamma_{Z_c(4200)\to J/\psi\pi} = 87.3$ MeV. Since the signal and background contribution do not interfere with each other as shown in the Dalitz plot, the signal of $Z_c^+(4200)$ can also be distinguished from the background. Thus, we can expect about $375/2$ GeV^2 events for the production of $J/\psi\pi^+$ in 50×10^6 collisions of γp at $W = 9.0$ GeV if taking $\Gamma_{Z_c(4200)\to J/\psi\pi} = 87.3$ MeV, which is enough to meet the requirements of the experiment. However, we also see that the signal of $Z_c^+(4200)$ is submerged in the background and will be difficult to distinguish from the background if taking $\Gamma_{Z_c(4200)\to J/\psi\pi} = 40.2$ MeV.

For comparison, we calculate the Dalitz plot and $J/\psi\pi^+$ invariant mass spectrum for the $\gamma p \to J/\psi\pi^+ n$ process without the Reggeized treatment at $W = 7.5$ GeV, as presented in Fig. 10. One finds that a vertical band related to the signal of $Z_c^+(4200)$ appears in the Dalitz plot even if the lowest partial decay width ($\Gamma_{Z_c(4200)\to J/\psi\pi} = 40.2$ MeV) is adopted, which is obviously different from that with Reggeized treatment.

IV. UPPER LIMIT OF THE DECAY WIDTH $\Gamma_{Z_c(4200)\to J/\psi\pi}$

The $J/\psi\pi^\pm$ mass spectrum presented by the COMPASS Collaboration in Ref. [56], which studied exclusive photoproduction of a $J/\psi\pi^\pm$ state at a nuclear target in the range from 7 to 19 GeV in the center-of-mass energy of the photon-nucleon system, does not exhibit any statistically

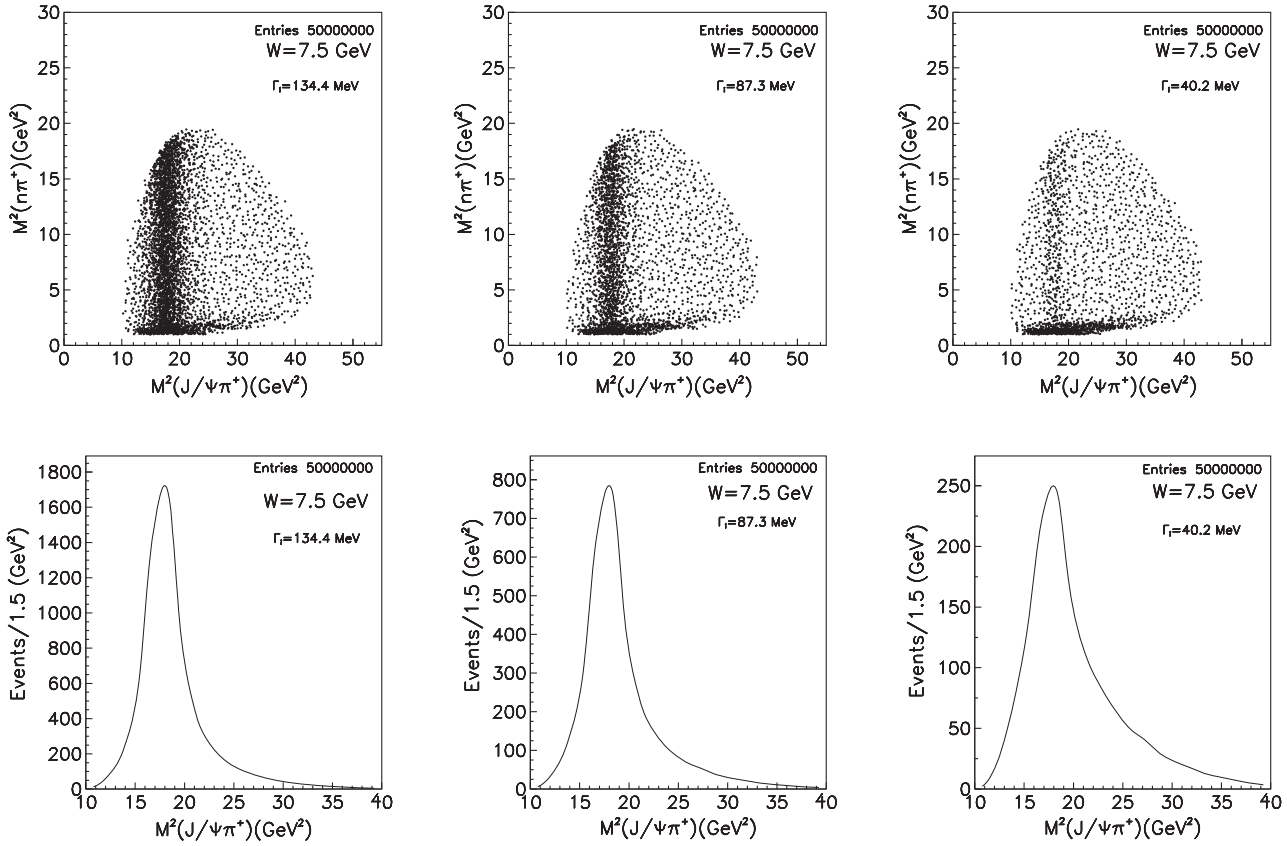

FIG. 10. The Dalitz plot (top) and the $J/\psi\pi^+$ invariant mass spectrum (bottom) for the $\gamma p \to J/\psi\pi^+ n$ reaction without the Reggeized treatment at center-of-mass energy $W = 7.5$ GeV. Here, the numerical results correspond to the partial decay width values $\Gamma_{Z(4200)\to J/\psi\pi} = 134.4$, 87.3, and 40.2 MeV.

significant structure at about 4.2 GeV. Nevertheless, it can be used for the estimation of an upper limit for the value $BR(Z_c(4200) \to J/\psi\pi) \times \sigma_{\gamma N \to Z_c(4200)N}$.

A sum of two exponential functions for a continuum and a Breit-Wigner curve for a possible contribution of $Z_c^{\pm}(4200)$ photoproduction was fitted to the mass spectrum in the range from 3.4 to 6.0 GeV. The mass $M_{Z_c(4200)} = 4196$ MeV and the width $\Gamma_{Z_c(4200)} = 370$ MeV were used as the fixed parameters. Doing this, we ignore the possible contribution of any other resonances like $Z_c(3900)$ and their interference with $Z_c(4200)$. The $J/\psi\pi^{\pm}$ mass spectrum with the fitting curve is shown in Fig. 11. The obtained from the fit possible number of $Z_c(4200)$ events is $N_{Z_c(4200)} = 58 \pm 31$. It can be converted to the upper limit $N^{UL}_{Z_c(4200)} < 98$ events corresponding to a confidence level of C.L. $= 90\%$. According to the normalization used in Ref. [56], this limit corresponds to the result

$$BR(Z_c(4200) \to J/\psi\pi) \times \sigma_{\gamma N \to Z_c(4200)N} < 340 \text{ pb}. \quad (27)$$

This result can be used for the estimation of an upper limit for the partial width $\Gamma_{J/\psi\pi}$ of the decay

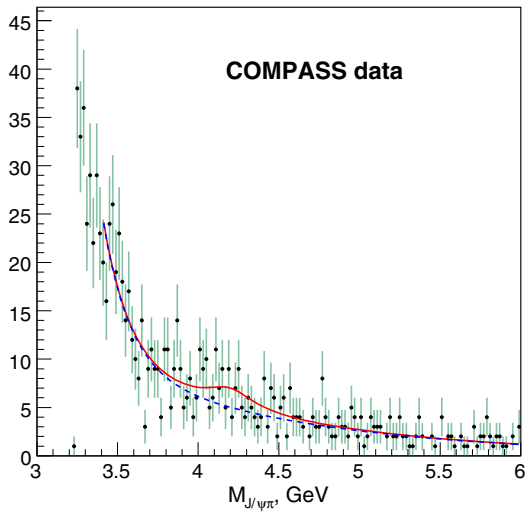

FIG. 11 (color online). Mass spectrum of the $J/\psi\pi$ state obtained by COMPASS [56]. The fitted function is shown as a red solid line. The dashed blue line corresponds to the continuum description.

$Z_c(4200) \to J/\psi\pi$ based on the Reggeized treatment. The production cross section, averaged over the W range covered by COMPASS, is about $\Gamma_{J/\psi\pi} \times 91$ pb/MeV. So

$$\frac{\Gamma_{J/\psi\pi}}{\Gamma_{\rm tot}} \times \sigma_{\gamma N \to Z_c^{\pm}(4200)N} = \frac{\Gamma_{J/\psi\pi}^2 \times 90 \text{ pb/MeV}}{\Gamma_{\rm tot}} < 340 \text{ pb}. \tag{28}$$

Assuming $\Gamma_{\rm tot} = 370$ MeV, we obtain an upper limit of $\Gamma_{J/\psi\pi} < 37$ MeV.

Photoproduction of the $Z_c^+(4200)$ state could also be tested by using the data on the HERMES experiment. It covers the range 2 GeV $< W <$ 6.3 GeV [86], where the difference between production cross sections calculated through pionic Regge trajectory exchange and virtual pion exchange is maximal.

V. SUMMARY

In this work, we study the charged $Z_c(4200)$ production in the $\gamma p \to J/\psi\pi^+ n$ reaction with an effective Lagrangian approach and the Regge trajectories model. Since the charmoniumlike $Z_c(4200)$ was observed only in the B meson decay process, it is an interesting and important topic to study the charmoniumlike $Z_c(4200)$ by different processes.

Through analysis and comparison, our numerical results indicate:

(I) The effect of introducing the Reggeized treatment has been to significantly reduce the magnitude of the cross section for $Z_c(4200)$ photoproduction. The total cross section for $\gamma p \to Z_c^+(4200)n$ via pionic Regge trajectory exchange is smaller than that without Reggeized treatment and the predictions in Refs. [52–55].

(II) We finds that the differential cross section for $\gamma p \to Z_c^+(4200)n$ by exchanging the pionic Regge trajectory is very sensitive to the θ angle and gives a considerable contribution at forward angles, which can be checked by further experiment and may be an effective way to examine the validity of the Reggeized treatment.

(III) The total cross section for the $\gamma p \to J/\psi\pi^+ n$ process with Reggeized treatment is lower than that without Reggeized treatment. The calculations indicate that the partial decay width $\Gamma_{Z_c(4200)\to J/\psi\pi}$ is a key parameter in studying the production of $Z_c(4200)$ via γp collision. Adopting the partial decay width predicted in Ref. [43] by assuming that the $Z_c(4200)$ is a tetraquark state, we find that the signal of $Z_c^+(4200)$ can also be distinguished from the background at $W = 9.0$ GeV if taking $\Gamma_{Z_c(4200)\to J/\psi\pi} = 87.3$ MeV, but not for the case of taking $\Gamma_{Z_c(4200)\to J/\psi\pi} = 40.2$ MeV. In Ref. [48], by assuming the $Z_c(4200)$ as an axial-vector moleculelike state, the partial decay width $\Gamma_{Z_c(4200)\to J/\psi\pi} = 24.6$ MeV was obtained with the QCD sum rule. If the predicted $\Gamma_{Z_c(4200)\to J/\psi\pi} = 24.6$ MeV in Ref. [48] is reliable, then the signal of $Z_c^+(4200)$ produced in the γp collision will be difficult to distinguish from the background. Thus, the experiment of the meson photoproduction of $Z_c(4200)$ may provide useful adjunctive information for the confirmation of the inner structure of $Z_c(4200)$.

(IV) The peak position of the total cross section for the $\gamma p \to Z_c^+(4200)n \to J/\psi\pi^+ n$ process was moved to the higher energy point when adding the Reggeized treatment, which means that a higher beam energy is necessary for the meson photoproduction of $Z_c(4200)$. The results show that $W \simeq 9.0$ GeV is the best energy window for searching for the $Z_c(4200)$ via γp collision. All these calculations can be checked in a future experiment.

(V) Using data on exclusive photoproduction of a $J/\psi\pi^{\pm}$ state from COMPASS, we estimated the upper limit for the value of a $Z_c(4200)$ production cross section multiplied by the branching ratio of the $Z_c(4200) \to J/\psi\pi$ decay to be above 340 pb (C.L. = 90%). According to the Reggeized treatment, it corresponds to the upper limit of $\Gamma_{Z_c(4200)\to J/\psi\pi}$ of about 37 MeV, which is coincident with the prediction of $\Gamma_{Z_c(4200)\to J/\psi\pi} = 24.6$ MeV by assuming the $Z_c(4200)$ as a moleculelike state in Ref. [48].

Since the Reggeized treatment used in this work has been proven to be more precise than the general effective Lagrangian approach in pion and kaon photoproduction [57–59], our theoretical results may provide valuable information, for both searching for the $Z_c(4200)$ via γp collision or explaining the lack of observation of $Z_c(4200)$ in experiment. Therefore, more experiments about the photoproduction of $Z_c(4200)$ are suggested, which will be important to improve our knowledge of the nature of $Z_c(4200)$ and the Regge theory.

ACKNOWLEDGMENTS

The authors acknowledge the COMPASS Collaboration for allowing us to use the data of the $J/\psi\pi^{\pm}$ mass spectrum. Meanwhile, X.-Y. W. is grateful to Dr. Qing-Yong Lin for valuable discussions and help. This work is partly supported by the National Basic Research Program (973 Program Grant No. 2014CB845406), the National Natural Science Foundation of China (Grant No. 11175220), and the One Hundred Person Project of the Chinese Academy of Science (Grant No. Y101020BR0).

[1] S. K. Choi *et al.* (Belle Collaboration), Phys. Rev. Lett. **91**, 262001 (2003).
[2] R. Aaij *et al.* (LHCb Collaboration), Phys. Rev. Lett. **110**, 222001 (2013).
[3] B. Aubert *et al.* (*BABAR* Collaboration), Phys. Rev. Lett. **95**, 142001 (2005).
[4] C. Z. Yuan *et al.* (Belle Collaboration), Phys. Rev. Lett. **99**, 182004 (2007).
[5] M. Ablikim *et al.* (BESIII Collaboration), Phys. Rev. Lett. **110**, 252001 (2013).
[6] Z. Q. Liu *et al.* (Belle Collaboration), Phys. Rev. Lett. **110**, 252002 (2013).
[7] M. Ablikim *et al.* (BESIII Collaboration), Phys. Rev. Lett. **112**, 132001 (2014).
[8] M. Ablikim *et al.* (BESIII Collaboration), Phys. Rev. Lett. **111**, 242001 (2013).
[9] R. Mizuk *et al.* (Belle Collaboration), Phys. Rev. D **78**, 072004 (2008).
[10] S. K. Choi *et al.* (Belle Collaboration), Phys. Rev. Lett. **100**, 142001 (2008).
[11] K. Chilikin *et al.* (Belle Collaboration), Phys. Rev. D **88**, 074026 (2013).
[12] R. Aaij *et al.* (LHCb Collaboration), Phys. Rev. Lett. **112**, 222002 (2014).
[13] K. Chilikin *et al.* (Belle Collaboration), Phys. Rev. D **90**, 112009 (2014).
[14] A. Bondar *et al.* (Belle Collaboration), Phys. Rev. Lett. **108**, 122001 (2012).
[15] I. Adachi *et al.* (Belle Collaboration), Phys. Rev. Lett. **108**, 032001 (2012).
[16] I. Adachi *et al.* (Belle Collaboration), arXiv:1105.4583.
[17] X. Liu, Chin. Sci. Bull. **59**, 3815 (2014).
[18] A. Esposito, A. L. Guerrieri, F. Piccinini, A. Pilloni, and A. D. Polosa, Int. J. Mod. Phys. A **30**, 1530002 (2015).
[19] S. L. Olsen, Hyperfine Interact. **229**, 7 (2014).
[20] M. Nielsen, F. S. Navarra, and S. H. Lee, Phys. Rep. **497**, 41 (2010).
[21] M. Nielsen and F. S. Navarra, Mod. Phys. Lett. A **29**, 1430005 (2014).
[22] T. Xiao, S. Dobbs, A. Tomaradze, and K. K. Seth, Phys. Lett. B **727**, 366 (2013).
[23] P. Krokovny *et al.* (Belle Collaboration), Phys. Rev. D **88**, 052016 (2013).
[24] M. Ablikim *et al.* (BESIII Collaboration), Phys. Rev. Lett. **113**, 212002 (2014).
[25] S. L. Zhu, Phys. Lett. B **625**, 212 (2005).
[26] Y.-R. Liu, M. Oka, M. Takizawa, X. Liu, W.-Z. Deng, and S.-L. Zhu, Phys. Rev. D **82**, 014011 (2010).
[27] N. Li and S.-L. Zhu, Phys. Rev. D **86**, 074022 (2012).
[28] H. Hogaasen, J. M. Richard, and P. Sorba, Phys. Rev. D **73**, 054013 (2006).
[29] D. Ebert, R. N. Faustov, and V. O. Galkin, Phys. Lett. B **634**, 214 (2006).
[30] N. Barnea, J. Vijande, and A. Valcarce, Phys. Rev. D **73**, 054004 (2006).
[31] Q. Wang, C. Hanhart, and Q. Zhao, Phys. Rev. Lett. **111**, 132003 (2013).
[32] E. Braaten, Phys. Rev. Lett. **111**, 162003 (2013).
[33] D. Y. Chen, X. Liu, and T. Matsuki, Phys. Rev. D **88**, 036008 (2013).
[34] C. F. Qiao and L. Tang, Eur. Phys. J. C **74**, 2810 (2014).
[35] F. Aceti, M. Bayar, and E. Oset, Eur. Phys. J. A **50**, 103 (2014).
[36] I. V. Danilkin, V. D. Orlovsky, and Yu. A. Simonov, Phys. Rev. D **85**, 034012 (2012).
[37] D. Bugg, Europhys. Lett. **96**, 11002 (2011).
[38] R. D. Matheus, S. Narison, M. Nielsen, and J.-M. Richard, Phys. Rev. D **75**, 014005 (2007).
[39] L. Maiani, F. Piccinini, A. D. Polosa, and V. Riquer, Phys. Rev. D **89**, 114010 (2014).
[40] L. Zhao, W. Z. Deng, and S. L. Zhu, Phys. Rev. D **90**, 094031 (2014).
[41] W. Chen and S. L. Zhu, Phys. Rev. D **83**, 034010 (2011).
[42] W. Chen and S. L. Zhu, Eur. Phys. J. Web Conf. **20**, 01003 (2012).
[43] W. Chen, T. G. Steele, H.-X. Chen, and S.-L. Zhu, Eur. Phys. J. C **75**, 358 (2015).
[44] J. J. Wu, R. Molina, E. Oset, and B. S. Zou, Phys. Rev. Lett. **105**, 232001 (2010).
[45] J. J. Wu, R. Molina, E. Oset, and B. S. Zou, Phys. Rev. C **84**, 015202 (2011).
[46] X. Y. Wang and X. R. Chen, Europhys. Lett. **109**, 41001 (2015).
[47] X. Y. Wang and X. R. Chen, Eur. Phys. J. A **51**, 85 (2015).
[48] Z. G. Wang, Int. J. Mod. Phys. A **30**, 1550168 (2015).
[49] H. W. Ke and X. Liu, Eur. Phys. J. C **58**, 217 (2008).
[50] X. Y. Wang, J. J. Xie, and X. R. Chen, Phys. Rev. D **91**, 014032 (2015).
[51] X. Y. Wang and X. R. Chen, Adv. High Energy Phys. **2015**, 918231 (2015).
[52] X. H. Liu, Q. Zhao, and F. E. Close, Phys. Rev. D **77**, 094005 (2008).
[53] J. He and X. Liu, Phys. Rev. D **80**, 114007 (2009).
[54] Q. Y. Lin, X. Liu, and H.-S. Xu, Phys. Rev. D **88**, 114009 (2013).
[55] Q. Y. Lin, X. Liu, and H.-S. Xu, Phys. Rev. D **89**, 034016 (2014).
[56] C. Adolph *et al.* (COMPASS Collaboration), Phys. Lett. B **742**, 330 (2015).
[57] M. Guidal, J. M. Laget, and M. Vanderhaeghen, Nucl. Phys. **A627**, 645 (1997).
[58] G. Galatá, Phys. Rev. C **83**, 065203 (2011).
[59] J. He, Phys. Rev. C **89**, 055204 (2014).
[60] A. B. Kaidalov, V. A. Khoze, A. D. Martin, and M. G. Ryskin, Eur. Phys. J. C **47**, 385 (2006).
[61] V. A. Khoze, A. D. Martin, and M. G. Ryskin, Eur. Phys. J. C **48**, 797 (2006).
[62] S. Chekanov *et al.* (ZEUS Collaboration), Nucl. Phys. **B637**, 3 (2002).
[63] B. Z. Kopeliovich, B. Povh, and I. Potashnikova, Z. Phys. C **73**, 125 (1996).
[64] H. Holtmann *et al.*, Phys. Lett. B **338**, 363 (1994).
[65] M. Burkardt, K. S. Hendricks, C.-R. Ji, W. Melnitchouk, and A. W. Thomas, Phys. Rev. D **87**, 056009 (2013).
[66] Y. Salamu, C.-R. Ji, W. Melnitchouk, and P. Wang, Phys. Rev. Lett. **114**, 122001 (2015).
[67] F. Carvalho *et al.*, arXiv:1507.07758.
[68] K. Tsushima, S. W. Huang, and A. Faessler, Phys. Lett. B **337**, 245 (1994).

[69] K. Tsushima, K. Saito, and A. W. Thomas, Phys. Lett. B **411**, 9 (1997); **421**, 413(E) (1998).
[70] K. Tsushima, A. Sibirtsev, A. W. Thomas, and G. Q. Li, Phys. Rev. C **59**, 369 (1999); **61**, 029903(E) (2000).
[71] Z. Lin, C. M. Ko, and B. Zhang, Phys. Rev. C **61**, 024904 (2000).
[72] K. A. Olive *et al.* (Particle Data Group), Chin. Phys. C **38**, 090001 (2014).
[73] T. Bauer and D. R. Yennie, Phys. Lett. **60B**, 165 (1976).
[74] T. Bauer and D. R. Yennie, Phys. Lett. **60B**, 169 (1976).
[75] T. H. Bauer, R. D. Spital, D. R. Yennie, and F. M. Pipkin, Rev. Mod. Phys. **50**, 261 (1978); **51**, 407(E) (1979).
[76] A. Donnachie and P. V. Landshoff, Phys. Lett. B **185**, 403 (1987).
[77] M. A. Pichowsky and T. S. H. Lee, Phys. Lett. B **379**, 1 (1996).
[78] V. P. Goncalves and M. L. L. da Silva, Phys. Rev. D **89**, 114005 (2014).
[79] R. J. Eden, Rep. Prog. Phys. **34**, 995 (1971).
[80] W. H. Liang, P. N. Shen, J. X. Wang, and B. S. Zou, J. Phys. G **28**, 333 (2002).
[81] R. Machleidt, K. Holinde, and Ch. Elster, Phys. Rep. **149**, 1 (1987).
[82] https://www.jlab.org/Hall-C/talks/08_21_06/Chudakov.pdf.
[83] A. Levy, arXiv:0711.0737.
[84] T. A. Armstrong *et al.*, Phys. Rev. Lett. **69**, 2337 (1992).
[85] M. Andreotti *et al.*, Phys. Rev. D **72**, 032001 (2005); D. Joffe, arXiv:hep-ex/0505007.
[86] A. Movsisyan, Eur. Phys. J. Web Conf. **73**, 02017 (2014).